JOURNAL OF MATERIALS SCIENCE 28 (1993) 982–988

Disordering of the Ni_3Si intermetallic compound by mechanical milling

J. S. C. JANG, C. H. TSAU
Materials Research Laboratories, Industrial Technology Research Institute, Hsinchu, Taiwan

The ordered f c c intermetallic compound Ni_3Si was mechanically milled in a high-energy ball mill. The severe plastic deformation produced by milling induced transformations with increasing milling time as follows: ordered f c c → disordered f c c → nanocrystalline f c c. The structural and microstructural evolution with milling time was followed by X-ray diffraction, TEM, hardness tests, and differential scanning calorimetry (DSC). Complete disordering occurred at milling times of 2 h and kept the saturated ΔH of the DSC peak in the range of estimated enthalpy even after 60 h milling. The structural development during milling of the f c c solid solution for Ni_3Si was presumably dominated by the formation and refinement of a dislocation cell structure into microcrystallites which eventually reached nanometre dimensions.

1. Introduction

The destabilization of crystalline material has recently become of interest in materials research. It has been shown that under certain thermodynamic and kinetic conditions the crystalline state is unstable and may collapse catastrophically into a disordered state [1, 2]. Crystal-to-glass transition has been achieved by rapid quenching, ion and electron irradiation, hydriding, and by solid state reaction in thin-film diffusion couples [1]. More recently, it was shown that grinding of a mixture of pure metals, mechanical alloying (MA) [3, 4], or of metal compounds, mechanical milling (MM) [5, 6], in a high-energy ball mill can result in amorphization.

The process of amorphization of elemental powders by MA has been explained by Schwarz and Koch [4] and Hellstern and Schultz [7] as the synthesis of an ultrafine composite in which a solid-state amorphizing reaction takes place, i.e. a method for producing fine-scale diffusion couples. The driving force for this reaction is the composition-induced destabilization of the crystalline phases in systems with large negative heats of mixing [8]. A kinetic constraint on formation of the equilibrum phase(s) is aided by asymmetry of the component diffusivities. On the other hand, the same result may be achieved by milling the pure intermetallic phase if sufficient energy can be stored in the crystalline compound in the form of grain boundaries, lattice and planar defects, and chemical disorder. Whereas this is possible for relatively complex crystal structures such as $NiTi_2$ [4] and $CuTi_2$ [9], it is difficult to achieve for simple crystal types, probably due to their effective recovery mechanisms at low temperatures. Recently, it has been shown for Ni_3Al ($L1_2$ type) [10] that ball milling results in only a crystal refinement of nanocrystalline dimensions and a partially amorphized phase, although the mechanically stored energy was comparable to the heat of crystallization for the amorphous alloy. In this study, we examined the stability of the Ni_3Si compound under heavy deformation by high-energy ball milling, and have compared the results with the same ordered f c c ($L1_2$ type) Ni_3Al intermetallic compound in order to determine the disordering mechanism of ordered f c c intermetallics.

2. Experimental procedure

The Ni_3Si intermetallic compound (Ni–24 at % Si) was prepared by arc melting together the appropriate amounts of nominally 99.99% pure nickel and electronic grade (99.999%) pure silicon under a partial pressure of pure argon, with a titanium getter. The compound buttons were crushed to powder form in a mortar and pestle, and the powder was annealed at 950 °C in a vacuum (4×10^{-6} torr; 1 torr = 133.322 Pa) for 2 h to ensure that it was a stress-free ordered $L1_2$ structure before milling. Mechanical milling was carried out in a Spex Mixer/Mill, model 8000, using a hardened tool steel vial and 440C martensitic balls (3.2 mm diameter). The vial was sealed with a viton O-ring in an argon-filled glove box, and the ball to powder weight ratio was 4:1. X-ray measurements were made with a Phillips diffractometer, model PW1710 with CuK_α ($\lambda = 0.1542$ nm) radiation. Oxygen analysis reveals oxygen contamination levels of less than 0.4 at % during milling. Thermal analyses were performed using a computerized differential scanning calorimeter (DSC), Du Pont 9900 thermal analyser. Microhardness was measured by a Akashi MVK-G1500 Microhardness tester at a load of 25 g on individual powder particles metallographically mounted. Eight measurements on each sample were collected to calculate the average values and standard deviation.

The microstructure evolution during MM was followed by both scanning (SEM) and transmission TEM electron microscopies. The morphology of the

0022–2461

free powders was examined in a CAMSCAN-530 SEM operated at 20 kV. Specimens for TEM were prepared by preparing powder pellet compacts (3 mm in diameter and 140–180 μm thick) by compressing the powder in a laboratory press under a pressure of 2 GPa. The compacted powder discs were thinned electromechanically in a Fischione Twin-Jet Electropolisher (model 110) in a solution of 10 vol % perchloric acid, 5 vol % hydrofluoric acid, 85 vol % methanol at a potential of 20–30 V. The polishing bath was maintained at a temperature of −25 °C. TEM was performed in a Jeol-2000FX microscope operating at 200 kV.

3. Results

The X-ray diffraction patterns of $Ni_{76}Si_{24}$ for selected milling times are presented in Fig. 1. The unmilled powder, after a stress-relief annealing at 950 °C for 2 h, exhibited relatively sharp diffraction lines for the $L1_2$ (ordered f c c) structure with a long-range-order (LRO) parameter, $S = 0.95$, although there was still a tiny Ni_5Si_2 phase coexisting in the Ni_3Si matrix. The intensity of the superlattice reflections decreased with milling time. The intensities of the fundamenral f c c lines also decreased with milling time and the width of the lines increased. The LRO parameter, S, was calculated in the usual way [11] from comparison of the integrated intensities of the superlattice lines. The results of ball milling the $Ni_{76}Si_{24}$ compound exhibit a monotonic decrease in S with milling time; $S = 0$ after 2 h milling time or greater, at which the superlattice reflections can no longer be resolved, shown as Fig. 2. At longer milling times the fundamental f c c lines continue to broaden, but are still present even after 24 h milling, as shown in Fig. 3. If the Scherrer formula is applied to the breadth of the major X-ray diffraction peak, the effective scattering length decreases with milling time and saturates at the value of 15 nm, as shown in Fig. 3. This is similar to the results of milling Ni_3Al compound, reported by Jang and Koch [10].

The change in the morphology of the powders with milling time was followed by scanning electron microscopy (SEM). The starting powder had a equiaxed blocky morphology as illustrated in Fig. 4. The sharp intergranular fracture morphology suggests

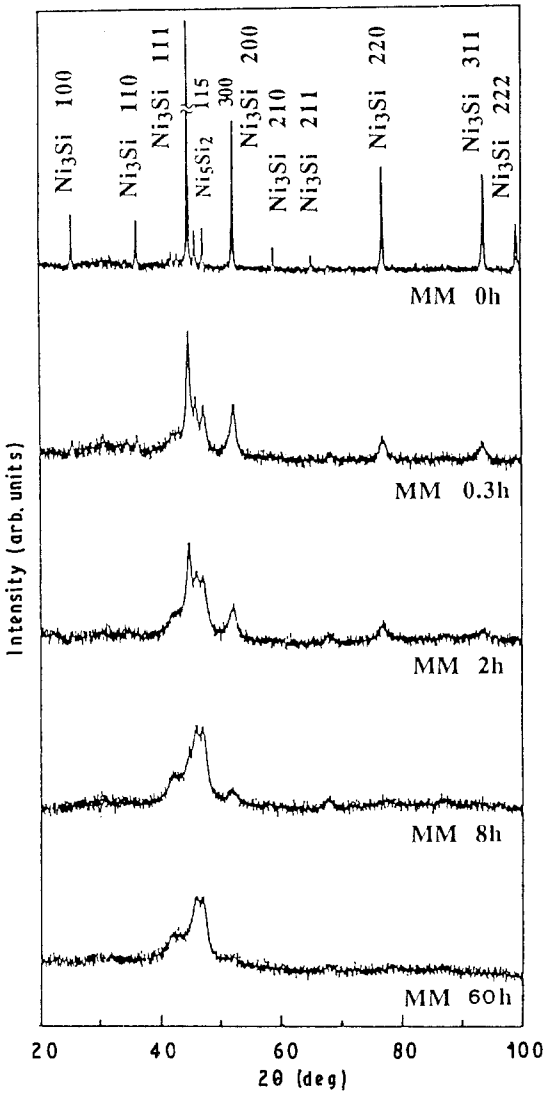

Figure 3 Crystal size as a function of milling time at room temperature for Ni_3Si. (○) X-ray diffraction, (●) TEM.

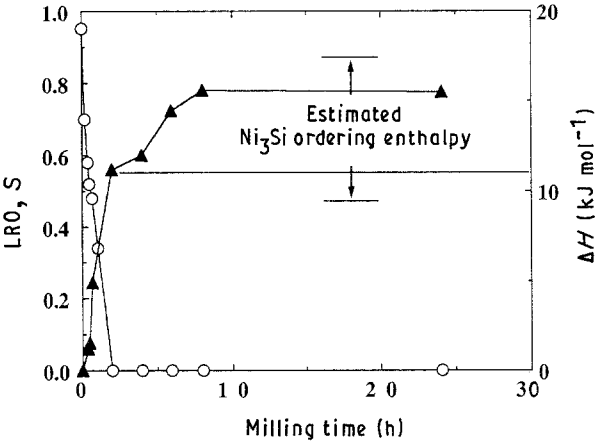

Figure 2 (○) Long-range order parameter, S, and (▲) enthalpy of the 430 °C DSC peak as a function of milling time for Ni_3Si milled at room temperature.

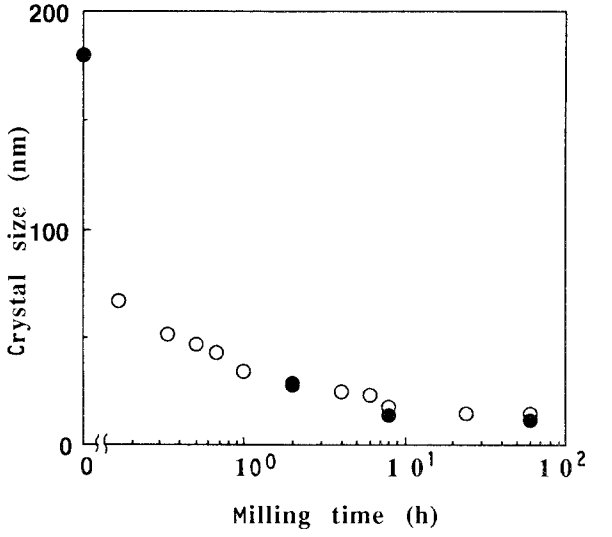

Figure 3 Crystal size as a function of milling time at room temperature for Ni_3Si. (○) X-ray diffraction (●) TEM.

cleavage fracture of the powder as prepared by crushing the as-cast buttons in the mortar and pestle. This general equiaxed blocky morphology is changed during milling with fragmentation of blocky fragments and rewelding of the fragments into still plate-like agglomerates. The morphology of the powder after milling for 2 h is as illustrated in Fig. 5. It is refined with further milling time as illustrated in Figs 6 and 7 for the samples milled for 8 and 60 h, respectively. The microstructures of the powder after various milling times were investigated by TEM. After 2 h milling a completely disordered f c c structure was observed in the selected-area diffraction pattern and the TEM observation revealed an image of sluggish severely deformed microstructure mixed with some fine equiaxed cell or grain structure, as illustrated in Fig. 8. The data for crystallite sizes measured in the TEM are plotted in Fig. 3 with the average coherent scattering distances determined from X-ray line broadening, using the Scherrer equation. Fair agreement for these quantities is observed at 8 and 60 h milling times, respectively. This is shown in Figs 9 and 10. It appears that a metastable equilibrium on the nanocrystalline grain/cell refinement is induced by the severe plastic deformation of ball milling. Meanwhile, no evidence is observed to reveal the amorphization of the Ni_3Si powder by ball milling.

The variation of microhardness of Ni_3Si with milling time is shown in Fig. 11; the microhardness is observed to rise rapidly with milling time and peak at 0.5 h. At this milling time the structure is heavily deformed and the LRO parameter, S, has decreased to about 0.6. According to the previous studies on the influence of LRO parameter on mechanical behaviour, it was found that the flow stress peaked in the Fe_3Al ordered intermetallic when the LRO parameter $S = 0.4$–0.6 [12]. This effect has been interpreted as due to the transition from deformation by superlattice dislocations in ordered structures to deformation by unit dislocations in the dislocation lattice. As disordering continues with milling time the hardness decreases again to a minimum value for the completely disordered f c c solid solution at 2 h, although the hardness here is still greater than the annealed, fully ordered powder. A small increase in hardness occurs on further milling and then the values appear

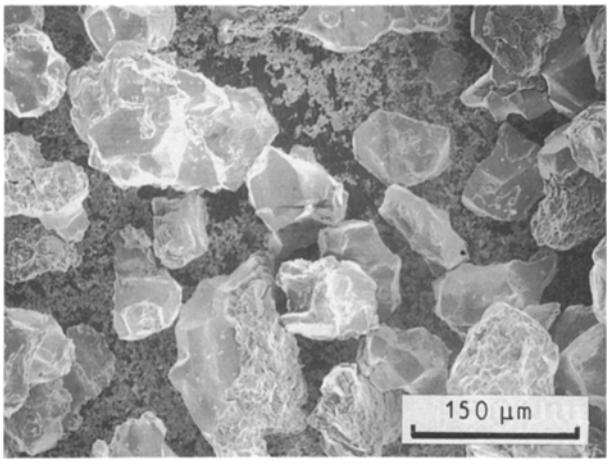

Figure 4 Scanning electron micrograph of starting Ni_3Si compound powder.

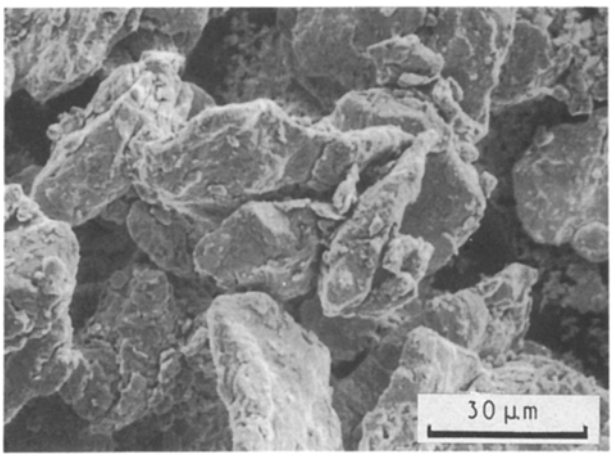

Figure 5 Scanning electron micrograph of Ni_3Si compound powder milled for 2 h.

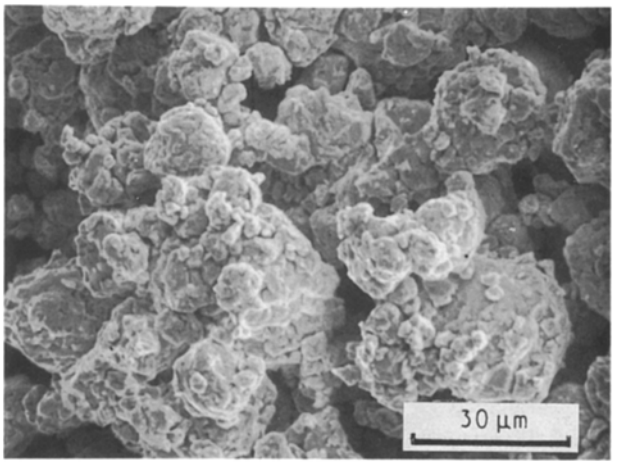

Figure 6 Scanning electron micrograph of Ni_3Si compound powder milled for 8 h.

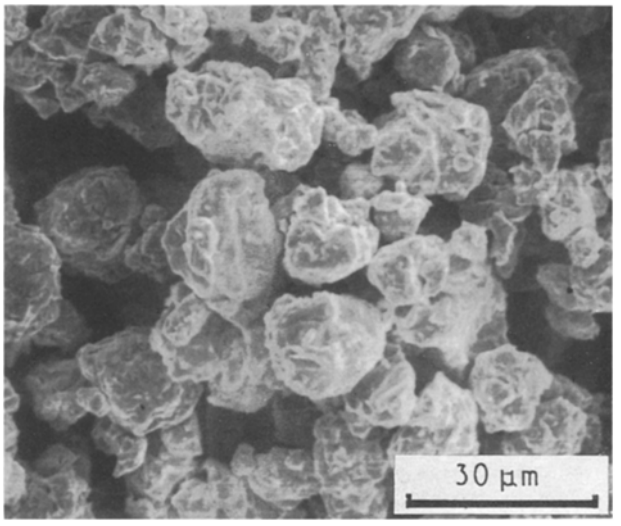

Figure 7 Scanning electron micrograph of Ni_3Si compound powder milled for 60 h.

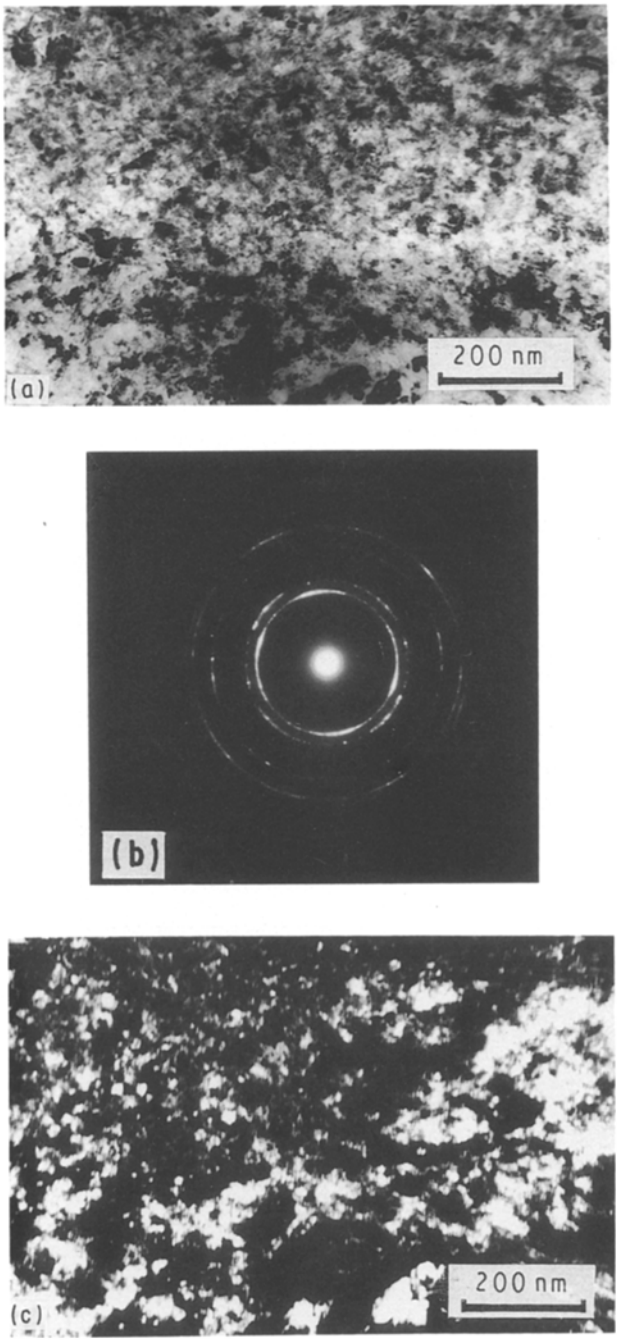

Figure 8 Transmission electron micrograph of Ni_3Si compound powder milled for 2 h: (a) bright-field image, (b) electron diffraction pattern, and (c) dark-field image of the (1 1 1) reflection.

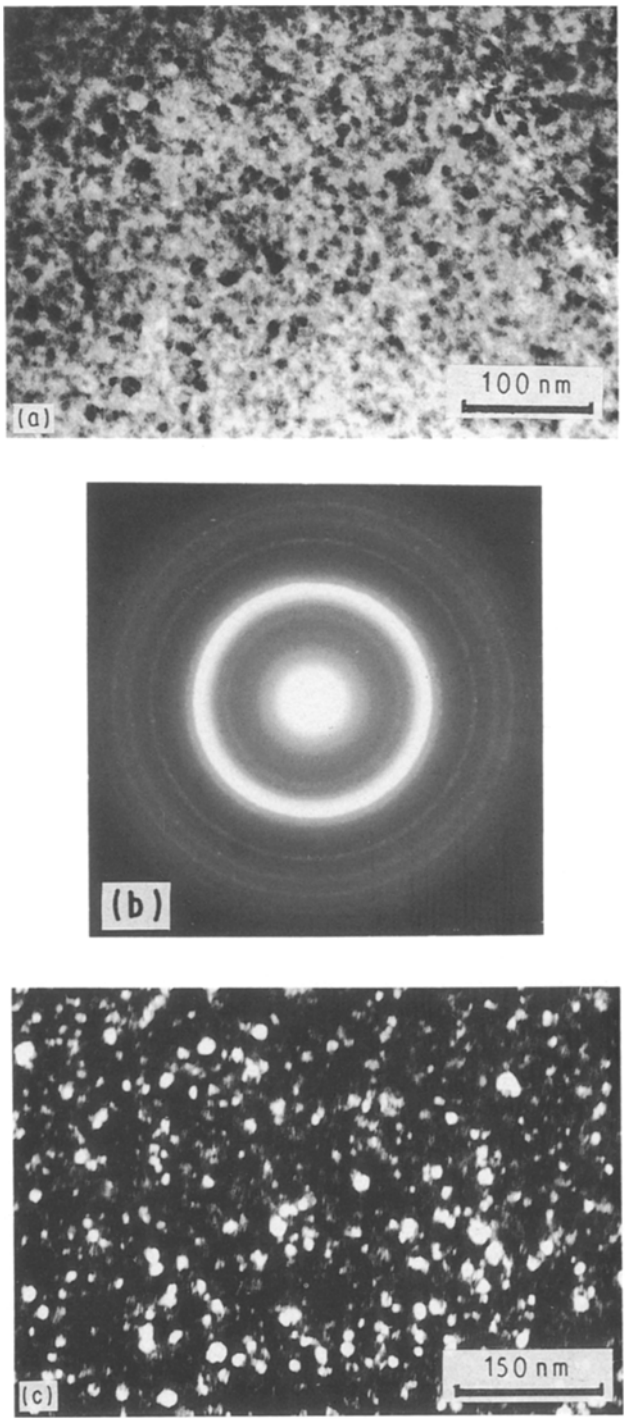

Figure 9 Transmission electron micrograph of Ni_3Si compound powder milled for 8 h: (a) bright-field image, (b) electron diffraction pattern, and (c) dark-field image of the (1 1 1) reflection.

to saturate to a constant level. This is presumably due to the effect of grain/cell refining and size saturation at about 12 nm.

The DSC measurements revealed an exothermic peak at about 430 °C which developed on milling Ni_3Si, as shown in Fig. 12. The measured enthalpies of the peak obtained from the calibrated integrated areas are plotted against milling time in Fig. 2. The peak enthalpy increases and reaches a saturation vaue of about 15.5 kJ mol^{-1} at about 6 h milling. A change in the slope of the monotonically increasing ΔH versus milling time curve for the 430 °C peak is evident at about 2 h, which is the milling time when the LRO disappears. The value estimated for the ordering enthalpy, shown as the horizontal line in Fig. 2, is consistent with the ΔH value ($\sim$ 11 kJ mol^{-1}) and time ($\sim$ 2 h) for the complete disordering of the $L1_2$ structure. The disordering enthalpy was estimated from the calculation by Kaufman of the heat of formation of Ni_3Si [13] and the observation of Luzzi and Meshii [14] that the ordering enthalpy for several ordered compounds is in the range of 21%–37% of the enthalpy of formation. The continued increase in ΔH of the peak for milling times after disordering is complete must be attributable to sources other than the enthalpy of the order–disorder transformation. Likely sources for the additional ΔH are presumably the

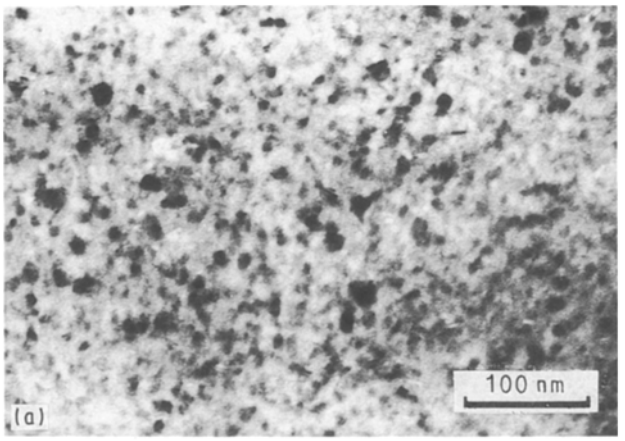

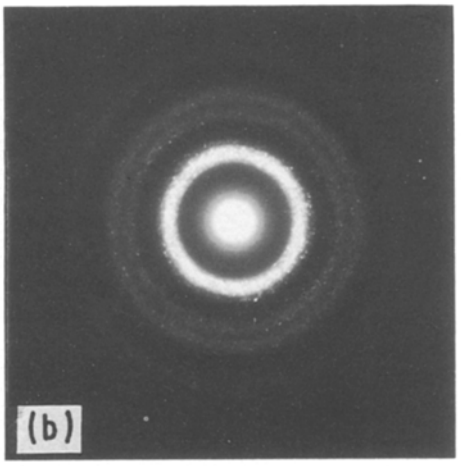

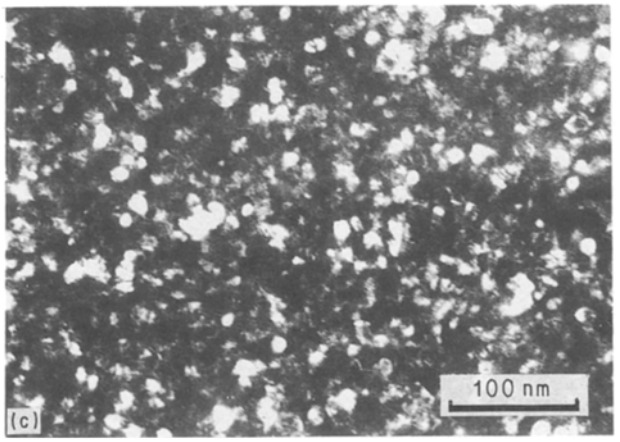

Figure 10 Transmission electron micrograph of Ni_3Si compound powder milled for 60 h: (a) bright-field image, (b) electron diffraction pattern, and (c) dark-field image of the (1 1 1) reflection.

release of stored energy of cold working in the form of reduced defect densities and crystallite coarsening.

4. Discussion

For any phase transformation, two considerations are always involved: (1) the thermodynamics of the system, i.e. the differences in free energies of the parent and product phase which is the driving free force, and (2) the kinetics, i.e. the mechanisms and constraints on the nucleation and growth of the product phase. Only one phase transition is evident in the present work on Ni_3Si that is introduced by the severe plastic deformation of high-energy ball milling, which is the order–disorder transition, $L1_2 \rightarrow fcc$.

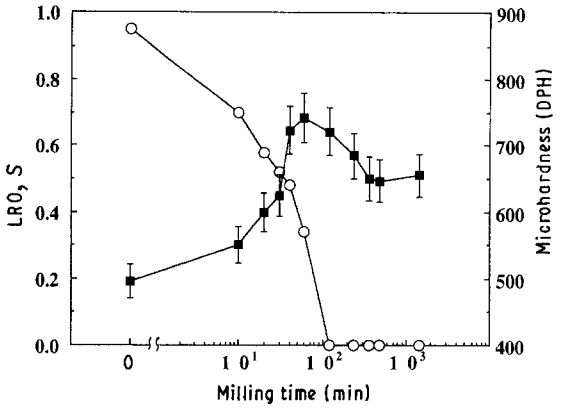

Figure 11 (○) Long-range order parameter, S, and (■) microhardness as a function of milling time for Ni_3Si milled at room temperature.

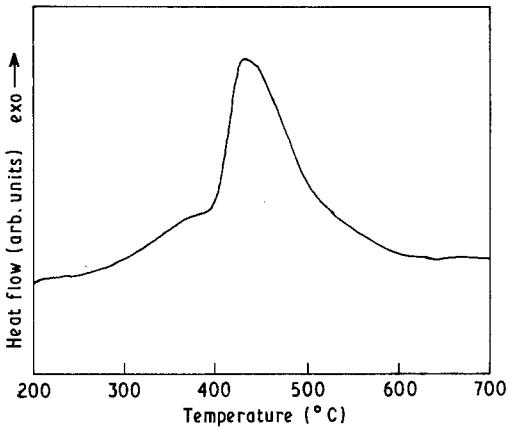

Figure 12 DSC scan for Ni_3Si powder milled at room temperature for 2 h.

In order to evaluate the thermodynamics of this transformation, a free-energy diagram for the Ni–Si system was constructed for a temperature of 300 K. A number of methods has been used to estimate the free energy of the phases, e.g. the CALPHAD approach [15]. Calculations of the enthalpy of formation which can be applied to estimate the free energy of intermediate phases include Miedema's model [16] and the embedded atom method [17]. These methods were used with standard thermodynamic relations to calculate the free energy diagram for Ni–Si at 300 K. The free energy curves for various stable and metastable phases in the Ni–Si system are given in Fig. 13. These values were calculated as follows. The free energies of the pure crystalline metals were referred to the gaseous state at 0 K and obtained from standard tables [18]. The free energies of the ideal solution of nickel and silicon are then given by $G^0 = X_{Ni}G^0_{Ni} + X_{Si}G^0_{Si}$ where $G^0_{Ni} = -370\,J\,mol^{-1}$, $G^0_{Si} = -245\,kJ\,mol^{-1}$. The difference between the free energy of the crystalline and amorphous (liquid) states, ΔG^{a-c}, for nickel and silicon was estimated from the expression introduced by Turnbull [19]

$$\Delta G^{a-c}(T) = \frac{\Delta H_f(T_M - T)}{T_M} \quad (1)$$

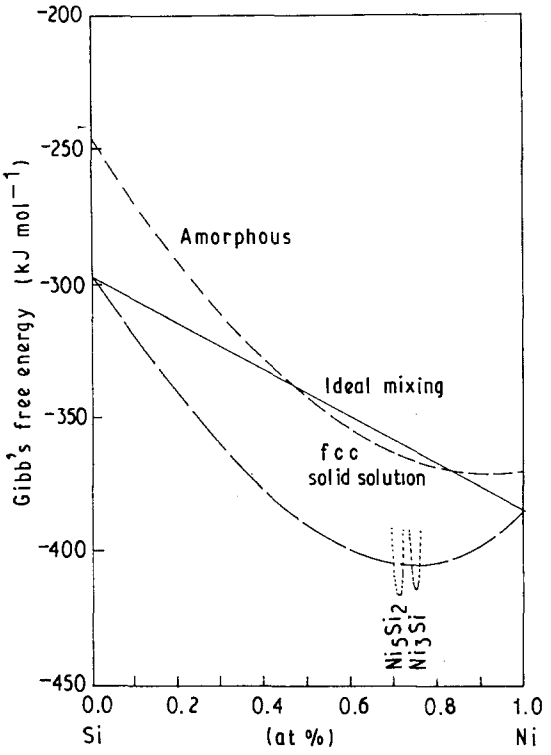

Figure 13 Calculated free-energy diagram for the Ni–Si alloy system.

where ΔH_f is the heat of fusion, T the temperature of interest, and T_M the melting temperature. Then the free energy of amorphous nickel and silicon is $(G^{a^0}_{Ni}, G^{a^0}_{Si})$ obtained from $G^{a^0}_{Ni} = \Delta G^{a-c}_{Ni} + G^0_{Ni}$, $G^{a^0}_{Si} = \Delta G^{a-c}_{Si} + G^0_{Si}$. The free energy of amorphous Ni–Si alloy is determined from the expressions

$$G^a_{Ni-Si} = G^{a^0}_{Ni-Si} + G^a_{mixing} \quad (2)$$

and

$$G^a_{mixing} = H^a_{mixing} - T \cdot S^a_{mixing}$$

where G^a_{mixing} is the free energy of mixing, H the enthalpy, S the entropy. The entropy of mixing is calculated assuming an ideal solution $S_{mixing} = R(X_{Ni} \ln X_{Ni} + X_{Si} \ln X_{Si})$ where R is the gas constant. H_{mixing} is estimated from Miedema's model adjusted for chemical short-range order [20, 21]. The free energies of the crystalline solid solutions were calculated from $G^{SS}_{Ni} = G^0_{Ni} + G^{mixing}_{Ni}$, $G^{SS}_{Si} = G^0_{Si} + G^{mixing}_{Si}$. G^{mixing}_{Ni}, G^{mixng}_{Si} can be obtained from the expressions derived by Kaufman and Nesor [13] for Ni–Si at 300 K. The free energies of the intermediate phases of the Ni–Si system were also calculated from the equations of Kaufman and Nesor [13]. These values were compared to those calculated from the Miedema's model. The free-energy diagram of Fig. 13 was then assembled from the above data and calculations. The free-energy diagram (Fig. 13) can now be used to help explain the phase transformations induced in Ni_3Si by ball milling.

While the LRO disappears, the ordering temperatures of MM Ni_3Si powder are consistent with the large exothermic peak observed in the DSC at $\approx 430\,^\circ C$, the enthalpy value for this peak (MM 2 h) is about 11.4 kJ mol^{-1}. This can be compared with the difference in free energy between the ordered and disordered fcc Ni_3Si of about 8.5 kJ mol^{-1}. From the free-energy curves of Fig. 13 and the estimates of the ordering enthalpy from enthalpy of formation for Ni_3Si which are in the range 9.5–16.7 kJ mol^{-1}, the entropy term in the free-energy calculations is small ($< 10\%\ \Delta H$) so the $\Delta G^{calc.}$ and $\Delta H^{exp.}$ values may be compared. Because the exothermic peak at 430 °C is presumably composed of more than the heat of the order–disorder transition, there appears to be good agreement between experimental and calculated ΔG values.

As noted in Section 1, in order for the equilibrium intermetallic compound to transform to an amorphous state, its free energy must be raised above that of the amorphous phase. In Ni_3Si, the total free energy change between the ordered fcc to the amorphous phase is estimated to be 50 kJ mol^{-1} (Fig. 13). The maximum change in enthalpy from the heavily deformed nanocrystaline fcc structure, as measured by DSC, to an ordered fcc crystalline phase is 15.5 kJ mol^{-1}. This value seems too low to drive the Ni_3Si from an ordered fcc to an amorphous structure. Meanwhile, the rate of dynamic recovery of Ni_3Si is probably higher than that of Ni_3Al. Therefore, the stored energy of Ni_3Si is much less than that of Ni_3Al under the same milling conditions. The microhardness also reaches a constant value at a short milling time of 2 h, suggesting that a dynamic equilibrium is reached between defect accumulation and recovery after the fully disordered state.

Jang and Koch [10] reported the partial amorphization of Ni_3Al intermetallic compound by high-energy ball milling. The microstructure after very high deformations was found to be formed of a cell structure of about 2 nm diameter. In some areas of the material, an image and selected-area electron diffraction pattern consistent with an amorphous structure were observed. Veprek *et al.* [22] also noted a crystalline-to-amorphous transition in silicon with decreasing grain size in chemical vapour deposited silicon films. An abrupt transition from microcrystalline to amorphous silicon was observed when the grain size was reduced to about 3 nm. Both Jang and Koch and Veprek *et al.* suggested that when the nanocrystalline grain size falls below some critical value, the increase in grain-boundary energy can act as the driving force for the crystalline-to-amorphous transformation. Because the Ni_3Si powder after long-term milling (8 h and longer), its grain (cell) size can only reach a saturated value of about 12 nm even after 60 h milling. This value is much higher than the assumed critical value of 2 nm. Comparing this result with the DSC enthalpy, implies that no amorphous phase will be obtained on the Ni_3Si in our ball milling. This is also analogous to the results currently obtained by Koch and colleagues [23].

5. Conclusions

High-energy ball milling can transform the ordered fcc Ni_3Si into a disordered fcc solid solution. The evolution of these transformations with milling time

was followed by X-ray diffraction, TEM, and DSC. Complete disordering occurred at milling times of 2 h and kept the saturated ΔH of the DSC peak in the range of estimated ordering enthalpy, even after 24 h milling. This differs from the results of energy storage for milling Ni_3Al; perhaps these two $L1_2$ compounds have different properties of dynamic recovery during mechanical milling. This may be the reason why the TEM observations only revealed an average grain diameter of 12 nm even after 60 h milling. However, the structural development during milling of the fcc solid solution for both Ni_3Si and Ni_3Al were analogous in being dominated by the formation and refinement of fine microcrystallites which eventually reached nanometre dimensions.

Acknowledgements

The authors thank Professor C. C. Koch for valuable discussions, Mr E. S. Pan for help with X-ray diffractometry, and Dr H. J. Lin for the computation of the free-energy calculation. The research reported in this paper was supported by the Ministry of Economic Affairs, the Republic of China.

References

1. W. L. JOHNSON, *Prog. Mater. Sci.* **30** (1986) 81.
2. W. L. JOHNSON and H. J. FECHT, *J. Less-Common Metals* **145** (1988) 63.
3. C. C. KOCH, O. B. CAVIN, C. G. McKAMEY and J. O. SCARBROUGH, *Appl. Phys. Lett.* **43** (1983) 1017.
4. R. B. SCHWARZ, R. R. PETRICH and C. K. SAW, *J. Non-Cryst. Solids* **76** (1985) 281.
5. A. E. ERMAKOV, E. E. YURCHIKOV and V. A. BARINOV, *Fiz. Metal. Metall.* **52** (1981).
6. R. B. SCHWARZ and C. C. KOCH, *Appl. Phys. Lett.* **49** (1986) 146.
7. E. HELLSTERN and L. SCHULTZ, *ibid.* **48** (1986) 124.
8. R. B. SCHWARZ and W. L. JOHNSON, *Phys. Rev. Lett.* **51** (1983) 415.
9. P. D. ASKENAZY, E. A. KAMENETZKY, L. E. TANNER and W. L. JOHNSON, *J. Less-Common Metals* **140** (1988) 149.
10. J. S. C. JANG and C. C. KOCH, *J. Mater. Res.* **5** (1989) 498.
11. B. D. CULLITY, "Elements of X-ray Diffraction" (Addison-Wesley, London, 1978) p. 386.
12. N. S. STOLOFF and R. G. DAVIES, *Prog. Mater. Sci.* **13** (1966) 3.
13. L. KAUFMAN, *CALPHAD* **3** (1979) 45.
14. D. E. LUZZI and M. MESHII, *Res. Mechanica* **21** (1987) 207.
15. L. KAUFMAN and H. BERNSTEIN, in "Computer Calculation of Phase Diagrams" (Academic Press, New York, 1970) Ch. 11.
16. A. R. MIEDEMA, *Philips Tech. Rev.* **36** (1976) 217.
17. M. S. DAW and M. I. BASKES, *Phys. Rev.* **B29** (1984) 6443.
18. R. C. WEAST, (ed.) "CRC Handbook of Chemistry and Physics" 65th Edn (CRC, Boca Raton, 1985) p. D-43.
19. D. TURNBULL, *J. Appl. Phys.* **21** (1950) 1122.
20. A. W. WEEBER, *J. Phys.* **F17** (1987) 809.
21. K. H. J. BUSCHOW, *J. Appl. Phys.* **56** (1984) 15.
22. S. VEPREK, Z. IQBAL and F. A. SAROTT, *Phil. Mag.* **B45** (1982) 137.
23. C. C. KOCH, in the workshop on "Fabrication Technologies and Applications of The High-Temperature Intermetallic Compounds," 16 May 1991 (Materials Research Laboratories, ITRI, Hsinchu, Taiwan) p. 1-1.

Received 15 October 1991
and accepted 25 June 1992